Electronic Supplementary Material (ESI) for CrystEngComm.

Supporting Information for

Luminescent Zn(II) coordination polymers as efficiently fluorescent sensors for highly sensitive detection of explosive nitroaromatics

Meng-Jung Tsai, Chih-Yu Li, and Jing-Yun Wu*

Department of Applied Chemistry, National Chi Nan University, Nantou 545, **T**aiwan. E-mail: jyunwu@ncnu.edu.tw

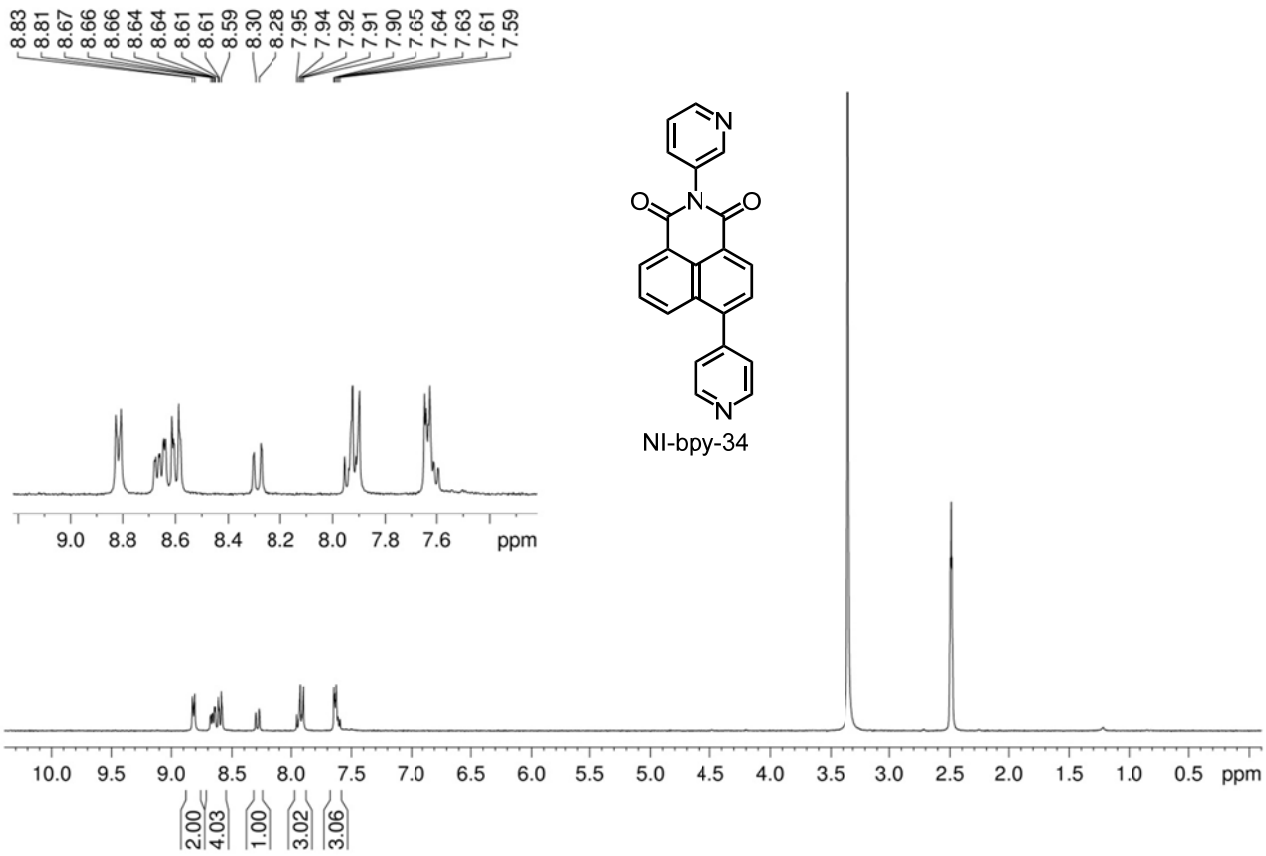

Fig. S1 ^{1}H NMR spectrum of NI-bpy-34 in DMSO-d_6.

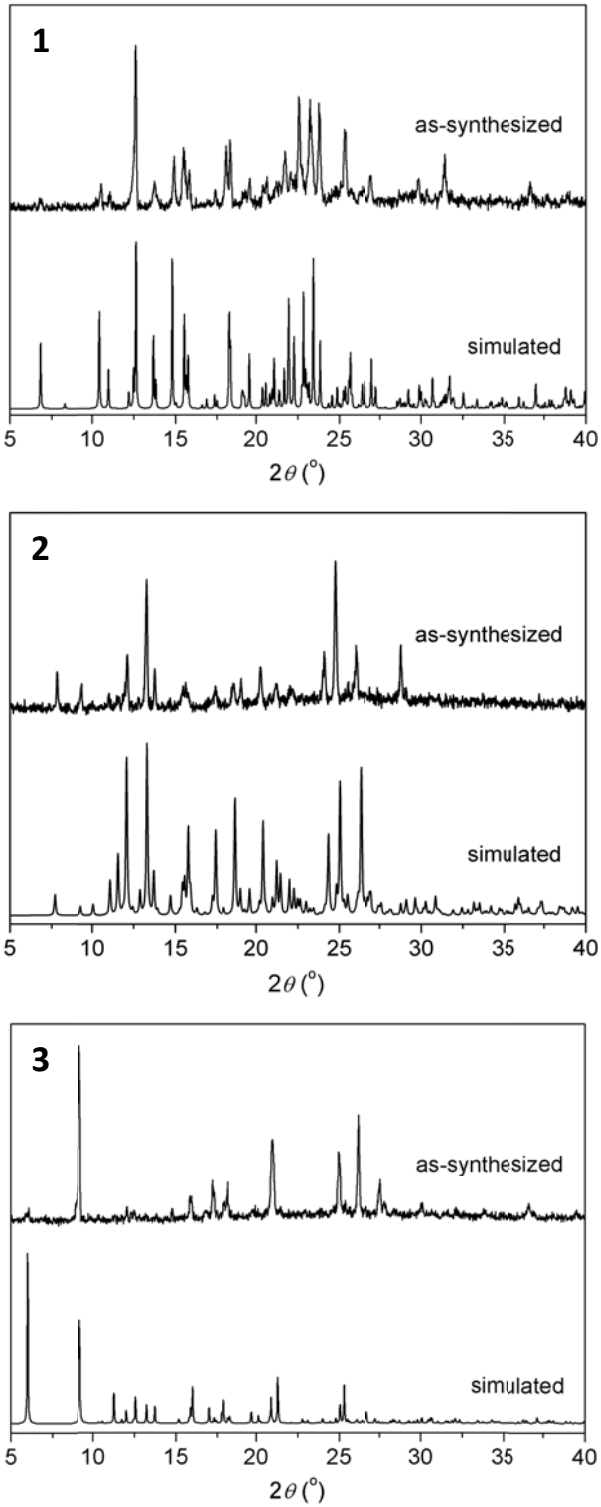

Fig. S2 XRPD patterns of **1**–**3**.

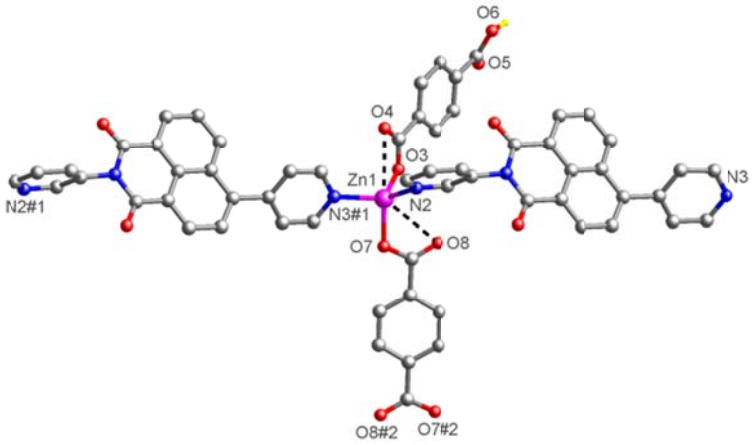

Fig. S3 Coordination environment around the Zn(II) center in **1**.

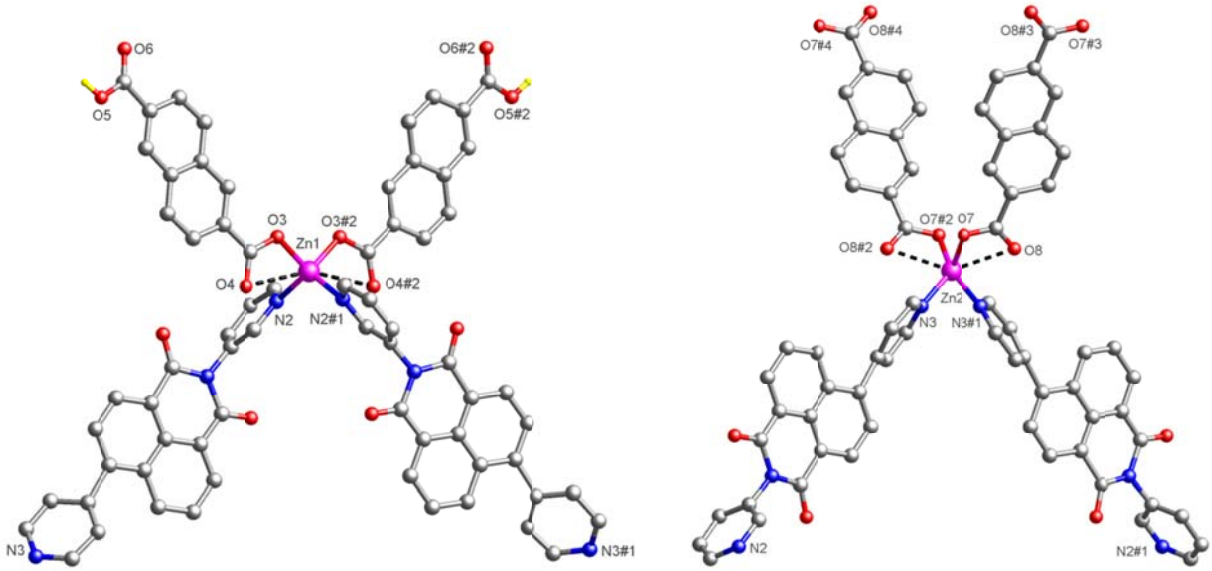

Fig. S4 Coordination environment around the Zn(II) center in **2**.

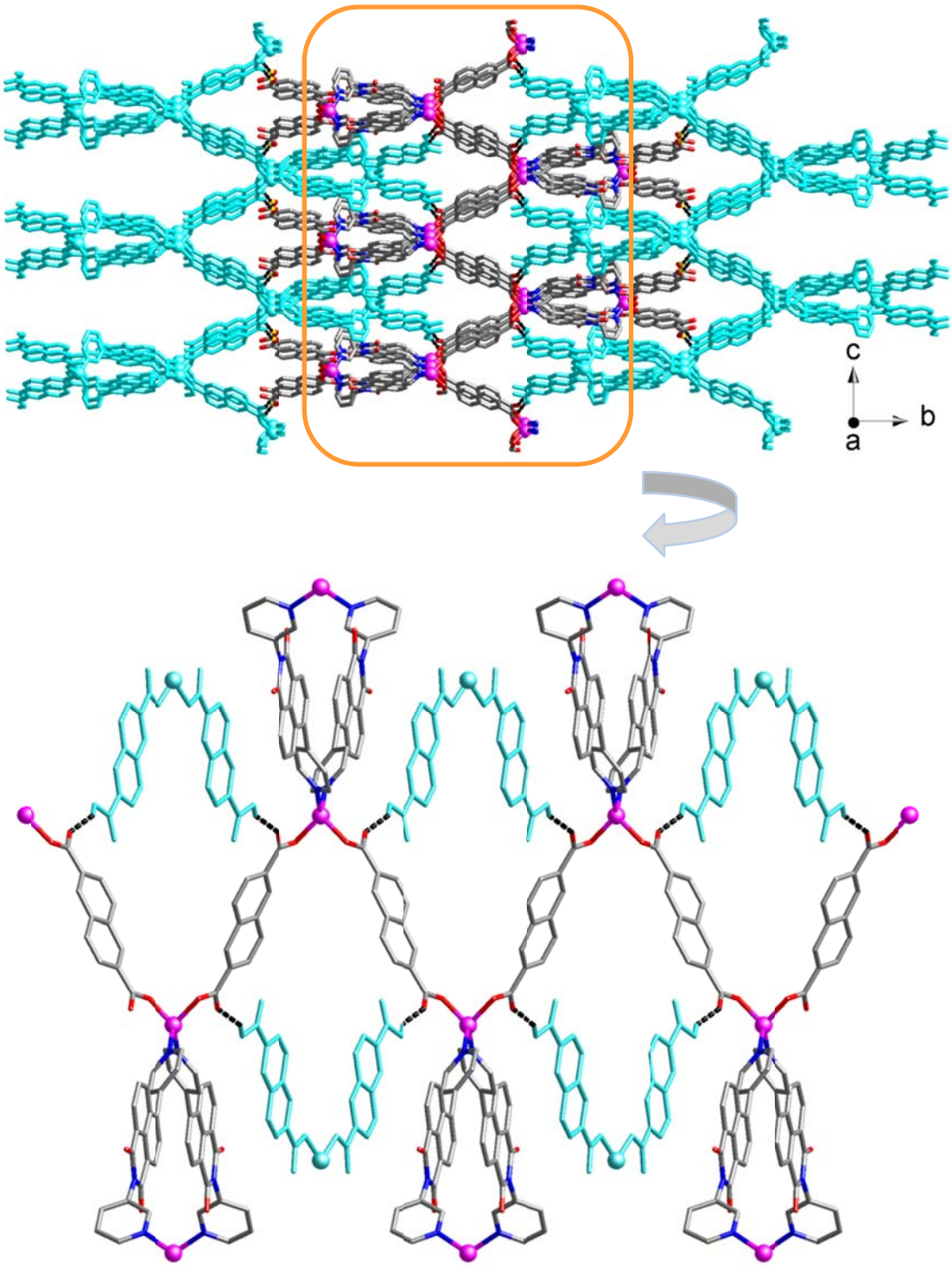

Fig. S5 Crystal structure of **2**: (top) view of the 3D H-bonded network slight off the crystallographic *a*-axis; (bottom) highlight of the layer-to-layer H-bonding interactions (black dash lines).

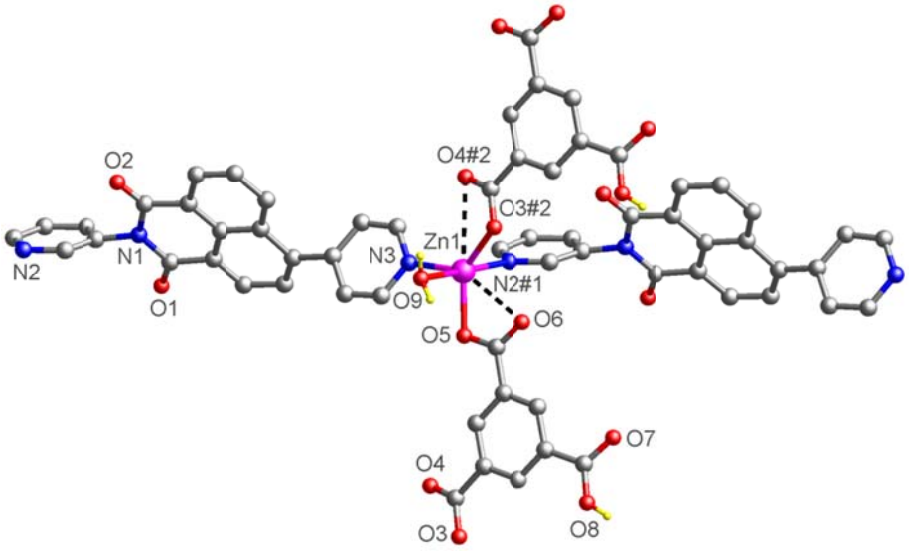

Fig. S6 Coordination environment around the Zn(II) center in **3**.

Table S1. Important hydrogen bond data for **1**–**3**[a]

D–H···A	*d*(D–H) [Å]	*d*(H···A) [Å]	*d*(D···A) [Å]	∠(D–H···A) [°]
		1		
O6–H101···O8#1	0.82	1.86	2.660(2)	165
		2		
O5–H5A···O8#1	0.84	1.90	2.587(15)	138
O9–H101···O2#2	0.81	2.29	2.984(12)	143
		3		
O8–H101···O11#1	0.83	1.66	2.483(16)	168
O8–H101···O15#1	0.83	2.57	3.36(2)	160
O9–H102···O3#2	0.90	1.92	2.754(6)	153
O9–H103···O6#2	0.83	1.93	2.682(6)	150

[a] Symmetry codes: For **1**: #1, –*x*, 1–*y*, 1–z; For **2**: #1, 1–*x*, 1–*y*, 1–z; #2, 1–*x*, *y*, 1/2–z; For **3**: #1, –1+*x*, *y*, 1+z; #2, –*x*, 1–*y*, –z.

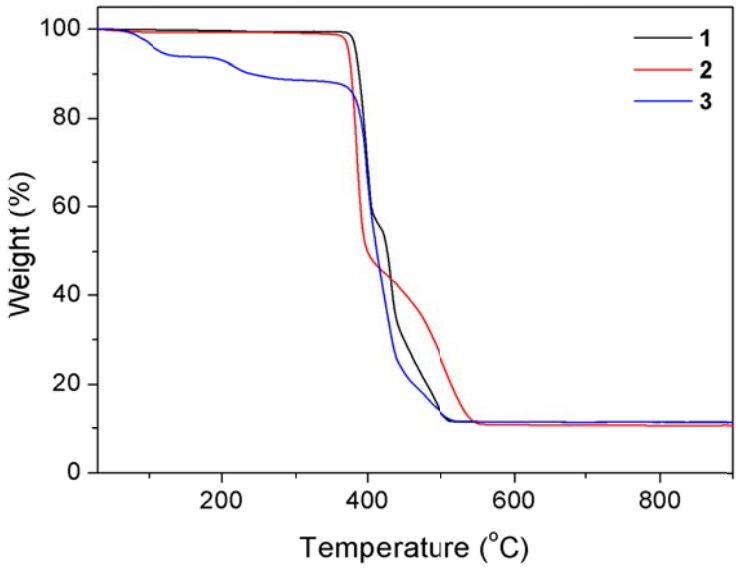

Fig. S7 TG diagrams of **1**–**3**.

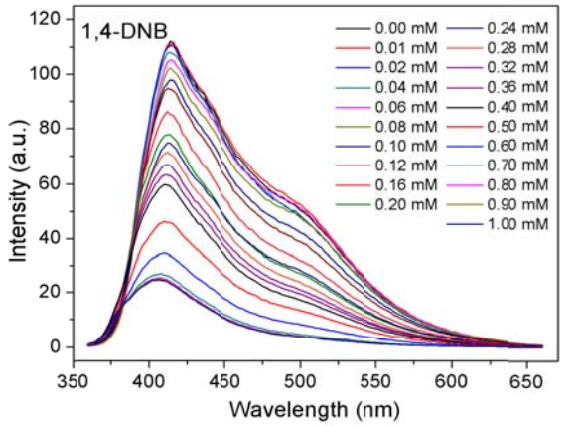
1,4-DNB
Intensity (a.u.)
Wavelength (nm)
0.00 mM
0.01 mM
0.02 mM
0.04 mM
0.06 mM
0.08 mM
0.10 mM
0.12 mM
0.16 mM
0.20 mM
0.24 mM
0.28 mM
0.32 mM
0.36 mM
0.40 mM
0.50 mM
0.60 mM
0.70 mM
0.80 mM
0.90 mM
1.00 mM

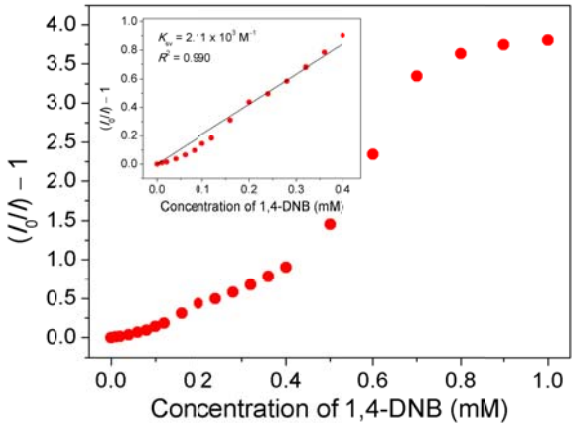
K_{sv} = 2.71 x 10^3 M^{-1}
R^2 = 0.990
$(I_0/I) - 1$
Concentration of 1,4-DNB (mM)

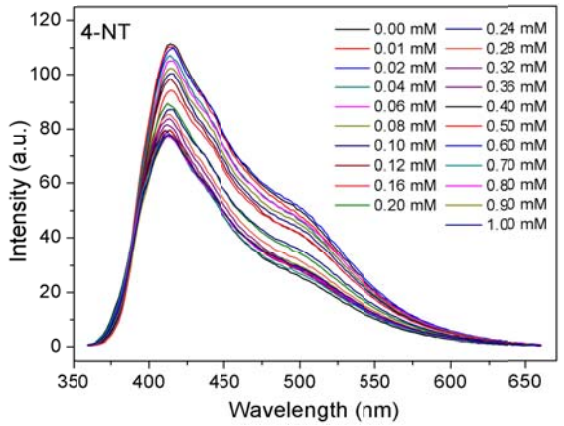
4-NT
Intensity (a.u.)
Wavelength (nm)
0.00 mM
0.01 mM
0.02 mM
0.04 mM
0.06 mM
0.08 mM
0.10 mM
0.12 mM
0.16 mM
0.20 mM
0.24 mM
0.28 mM
0.32 mM
0.36 mM
0.40 mM
0.50 mM
0.60 mM
0.70 mM
0.80 mM
0.90 mM
1.00 mM

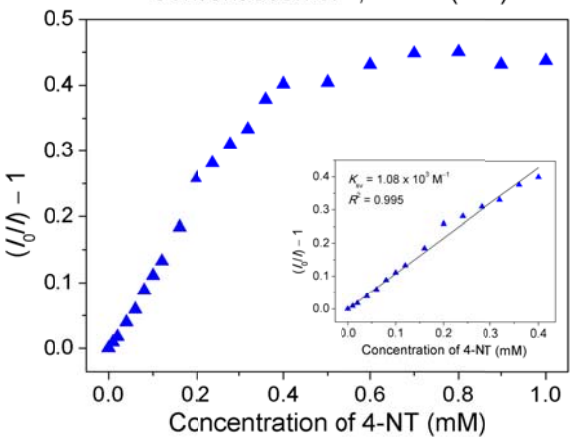
K_{sv} = 1.08 x 10^3 M^{-1}
R^2 = 0.995
$(I_0/I) - 1$
Concentration of 4-NT (mM)

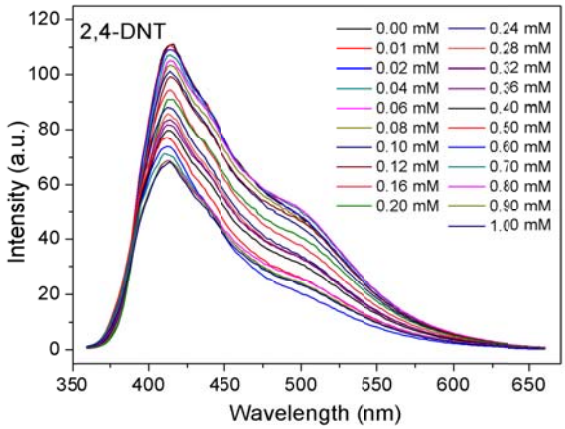
2,4-DNT
Intensity (a.u.)
Wavelength (nm)
0.00 mM
0.01 mM
0.02 mM
0.04 mM
0.06 mM
0.08 mM
0.10 mM
0.12 mM
0.16 mM
0.20 mM
0.24 mM
0.28 mM
0.32 mM
0.36 mM
0.40 mM
0.50 mM
0.60 mM
0.70 mM
0.80 mM
0.90 mM
1.00 mM

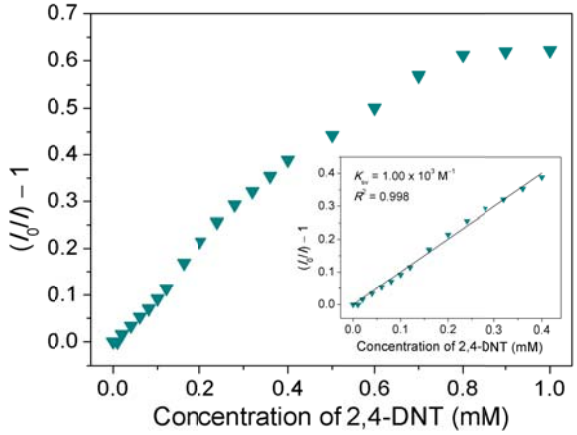
K_{sv} = 1.00 x 10^3 M^{-1}
R^2 = 0.998
$(I_0/I) - 1$
Concentration of 2,4-DNT (mM)

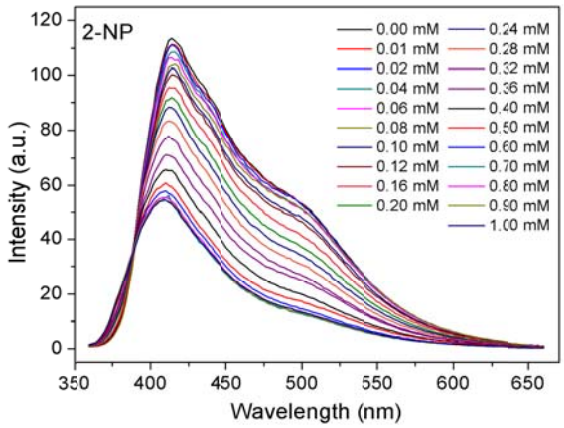
2-NP
Intensity (a.u.)
Wavelength (nm)
0.00 mM
0.01 mM
0.02 mM
0.04 mM
0.06 mM
0.08 mM
0.10 mM
0.12 mM
0.16 mM
0.20 mM
0.24 mM
0.28 mM
0.32 mM
0.36 mM
0.40 mM
0.50 mM
0.60 mM
0.70 mM
0.80 mM
0.90 mM
1.00 mM

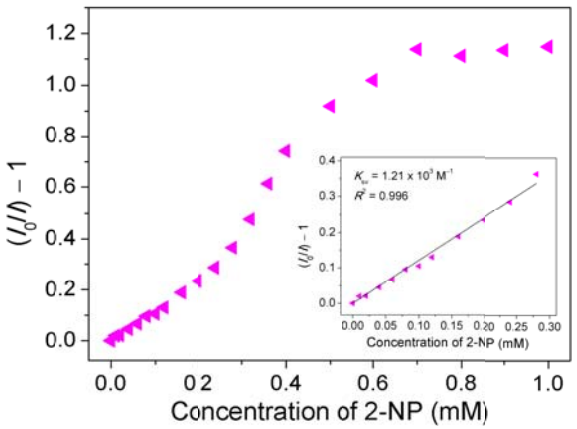
K_{sv} = 1.21 x 10^3 M^{-1}
R^2 = 0.996
$(I_0/I) - 1$
Concentration of 2-NP (mM)

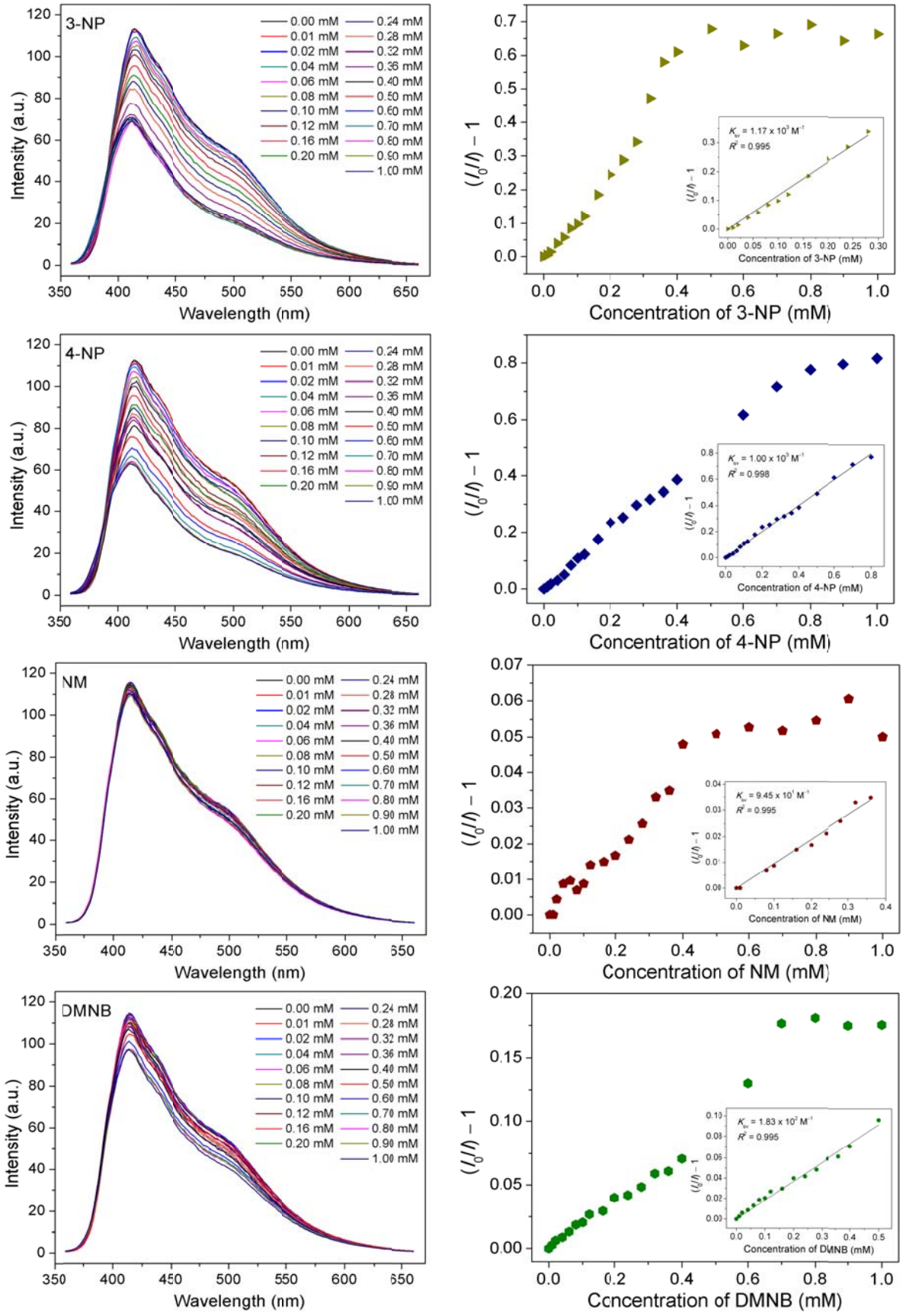

Fig. S8 (Left) Fluorescence responses of **1** in toluene suspension (3.0 mg/3 mL) toward different concentrations of different nitro analyte. (Right) Stern–Volmer plot for nitro analyte in the presence of toluene suspension of **1** in the range from 0 to 1.00 mM. Inset shows the linear region for Stern–Volmer analysis of **1** as a function of concentration of nitro analyte.

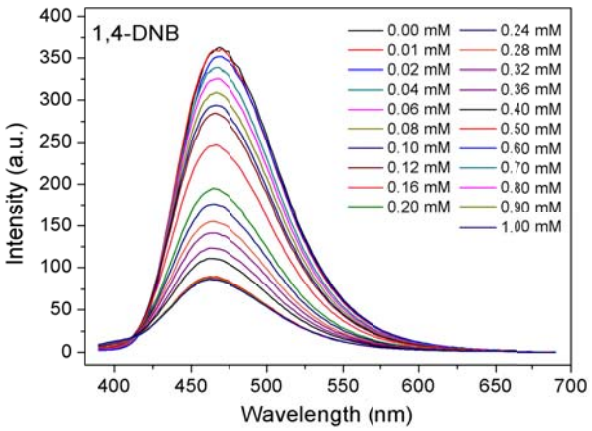
1,4-DNB
Intensity (a.u.)
Wavelength (nm)
0.00 mM
0.01 mM
0.02 mM
0.04 mM
0.06 mM
0.08 mM
0.10 mM
0.12 mM
0.16 mM
0.20 mM
0.24 mM
0.28 mM
0.32 mM
0.36 mM
0.40 mM
0.50 mM
0.60 mM
0.70 mM
0.80 mM
0.90 mM
1.00 mM

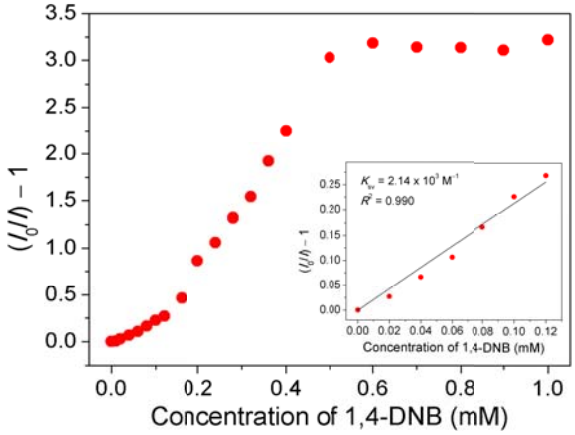
$(I_0/I) - 1$
Concentration of 1,4-DNB (mM)
K_{sv} = 2.14 x 10^3 M^{-1}
R^2 = 0.990
Concentration of 1,4-DNB (mM)

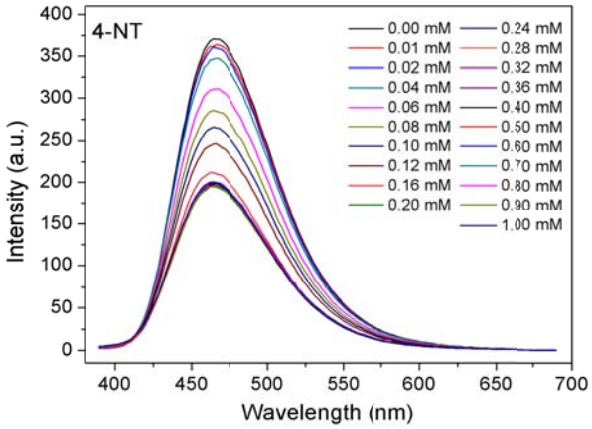
4-NT
Intensity (a.u.)
Wavelength (nm)
0.00 mM
0.01 mM
0.02 mM
0.04 mM
0.06 mM
0.08 mM
0.10 mM
0.12 mM
0.16 mM
0.20 mM
0.24 mM
0.28 mM
0.32 mM
0.36 mM
0.40 mM
0.50 mM
0.60 mM
0.70 mM
0.80 mM
0.90 mM
1.00 mM

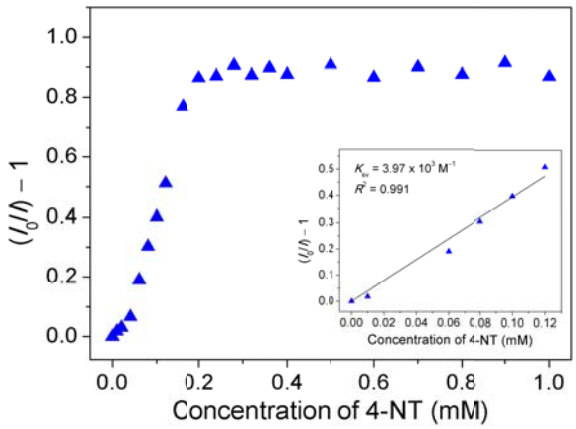
$(I_0/I) - 1$
Concentration of 4-NT (mM)
K_{sv} = 3.97 x 10^3 M^{-1}
R^2 = 0.991
Concentration of 4-NT (mM)

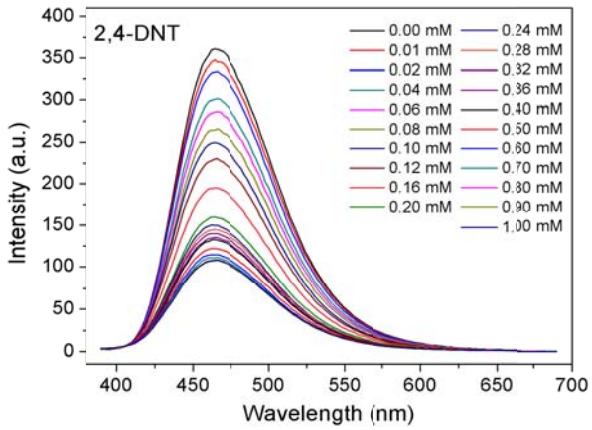
2,4-DNT
Intensity (a.u.)
Wavelength (nm)
0.00 mM
0.01 mM
0.02 mM
0.04 mM
0.06 mM
0.08 mM
0.10 mM
0.12 mM
0.16 mM
0.20 mM
0.24 mM
0.28 mM
0.32 mM
0.36 mM
0.40 mM
0.50 mM
0.60 mM
0.70 mM
0.80 mM
0.90 mM
1.00 mM

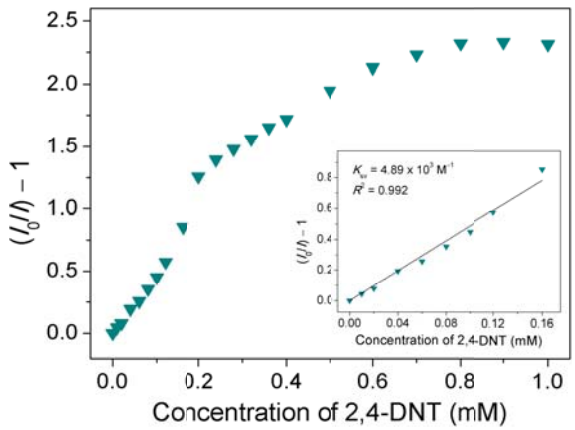
$(I_0/I) - 1$
Concentration of 2,4-DNT (mM)
K_{sv} = 4.89 x 10^3 M^{-1}
R^2 = 0.992
Concentration of 2,4-DNT (mM)

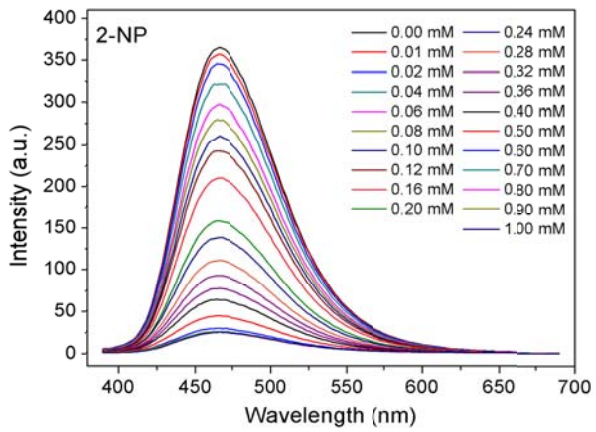
2-NP
Intensity (a.u.)
Wavelength (nm)
0.00 mM
0.01 mM
0.02 mM
0.04 mM
0.06 mM
0.08 mM
0.10 mM
0.12 mM
0.16 mM
0.20 mM
0.24 mM
0.28 mM
0.32 mM
0.36 mM
0.40 mM
0.50 mM
0.60 mM
0.70 mM
0.80 mM
0.90 mM
1.00 mM

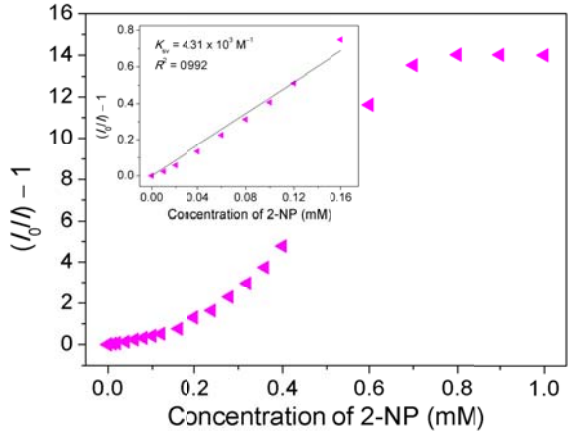
$(I_0/I) - 1$
Concentration of 2-NP (mM)
K_{sv} = 4.31 x 10^3 M^{-1}
R^2 = 0992
Concentration of 2-NP (mM)

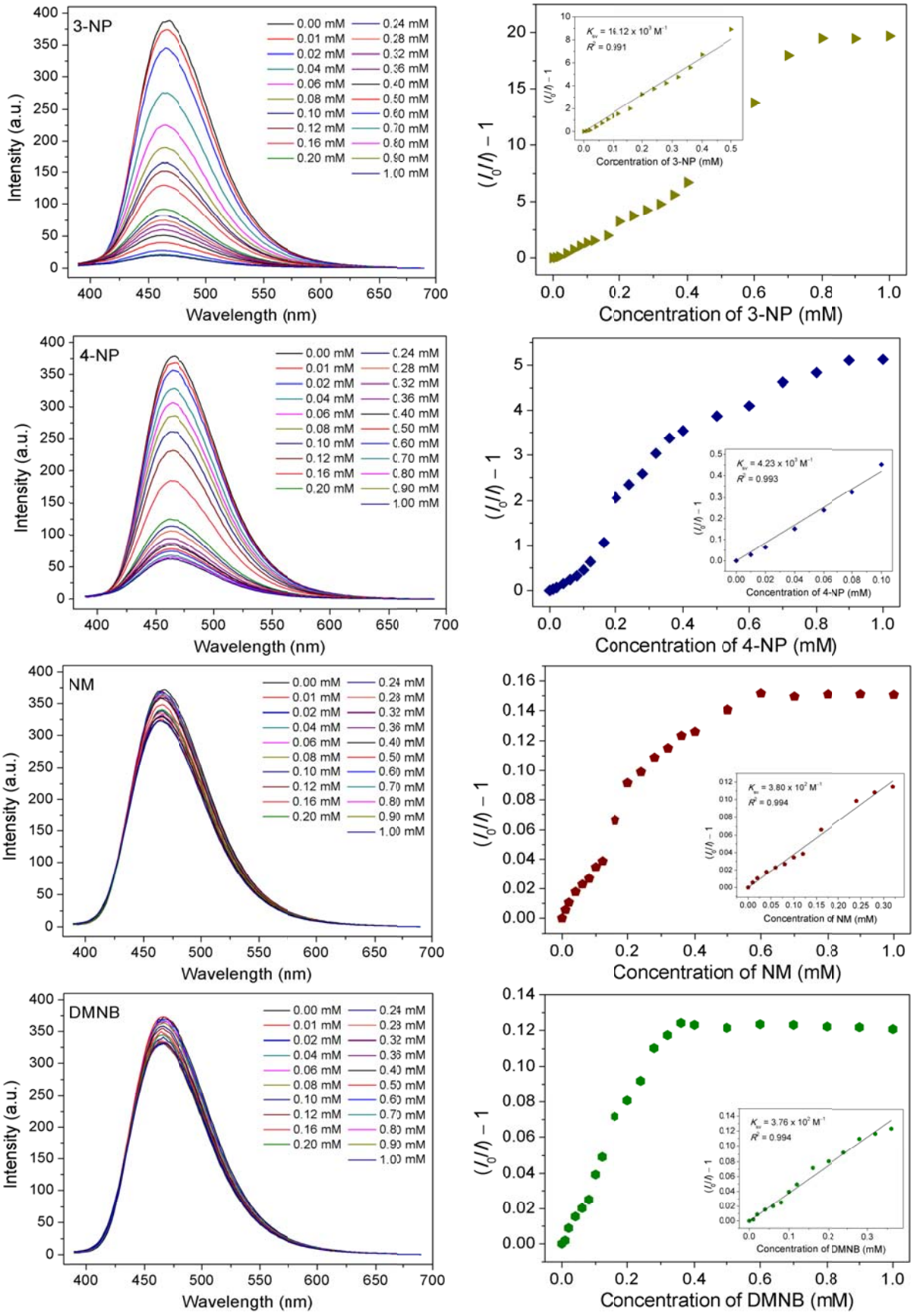

Fig. S9 (Left) Fluorescence responses of **2** in toluene suspension (3.0 mg/3 mL) toward different concentrations of different nitro analyte. (Right) Stern–Volmer plot for nitro analyte in the presence of toluene suspension of **2** in the range from 0 to 1.00 mM. Inset shows the linear region for Stern–Volmer analysis of **2** as a function of concentration of nitro analyte.

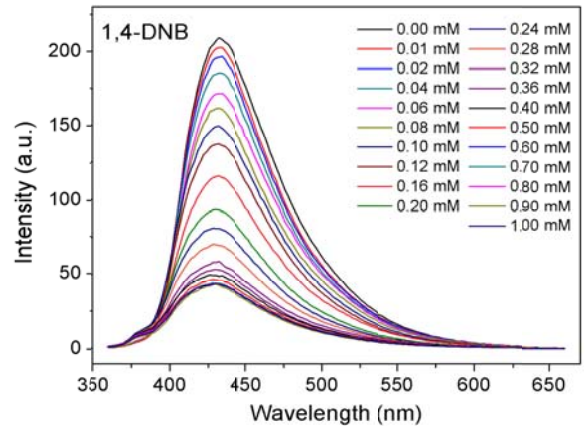
1,4-DNB
Intensity (a.u.)
Wavelength (nm)
0.00 mM
0.01 mM
0.02 mM
0.04 mM
0.06 mM
0.08 mM
0.10 mM
0.12 mM
0.16 mM
0.20 mM
0.24 mM
0.28 mM
0.32 mM
0.36 mM
0.40 mM
0.50 mM
0.60 mM
0.70 mM
0.80 mM
0.90 mM
1.00 mM

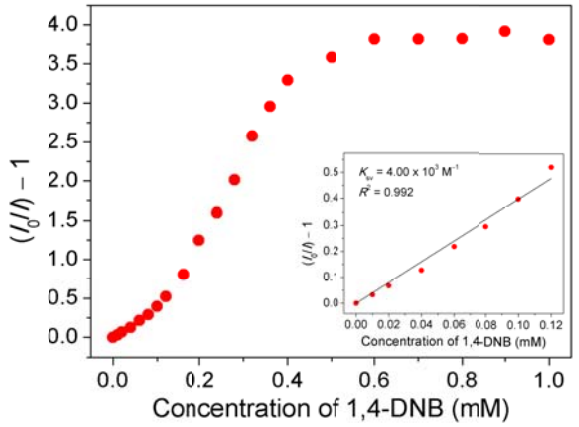
$(I_0/I) - 1$
Concentration of 1,4-DNB (mM)
K_{sv} = 4.00 x 10^3 M^{-1}
R^2 = 0.992

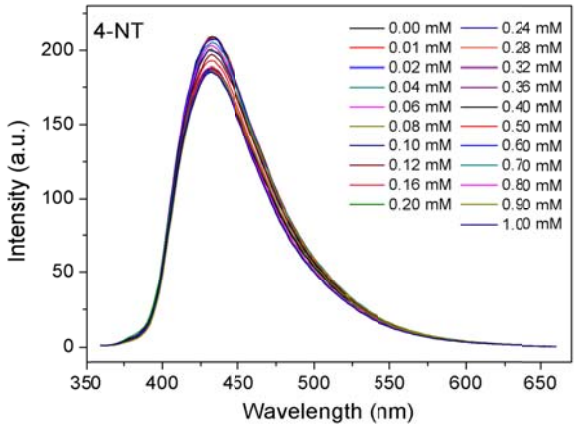
4-NT
Intensity (a.u.)
Wavelength (nm)
0.00 mM
0.01 mM
0.02 mM
0.04 mM
0.06 mM
0.08 mM
0.10 mM
0.12 mM
0.16 mM
0.20 mM
0.24 mM
0.28 mM
0.32 mM
0.36 mM
0.40 mM
0.50 mM
0.60 mM
0.70 mM
0.80 mM
0.90 mM
1.00 mM

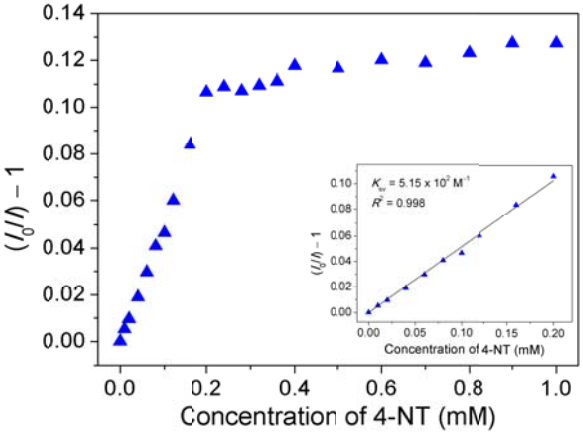
$(I_0/I) - 1$
Concentration of 4-NT (mM)
K_{sv} = 5.15 x 10^2 M^{-1}
R^2 = 0.998

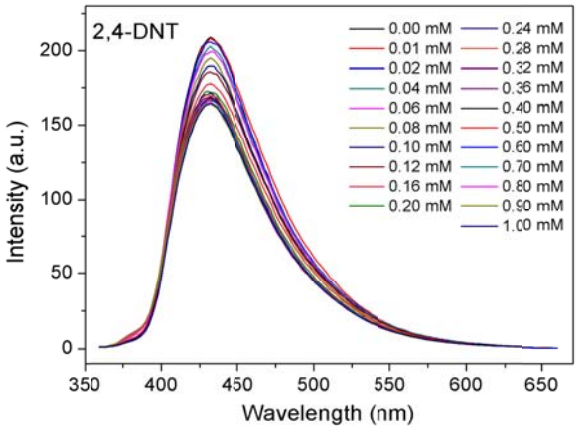
2,4-DNT
Intensity (a.u.)
Wavelength (nm)
0.00 mM
0.01 mM
0.02 mM
0.04 mM
0.06 mM
0.08 mM
0.10 mM
0.12 mM
0.16 mM
0.20 mM
0.24 mM
0.28 mM
0.32 mM
0.36 mM
0.40 mM
0.50 mM
0.60 mM
0.70 mM
0.80 mM
0.90 mM
1.00 mM

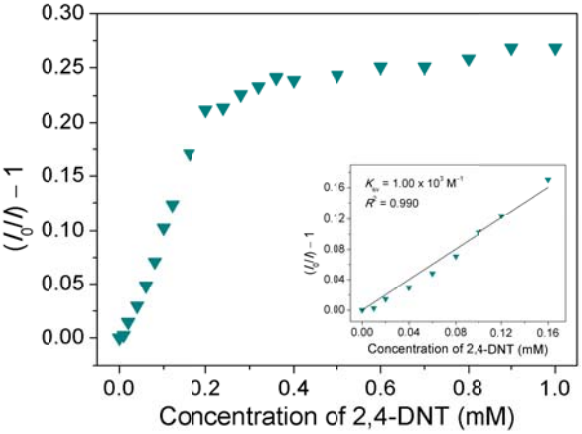
$(I_0/I) - 1$
Concentration of 2,4-DNT (mM)
K_{sv} = 1.00 x 10^3 M^{-1}
R^2 = 0.990

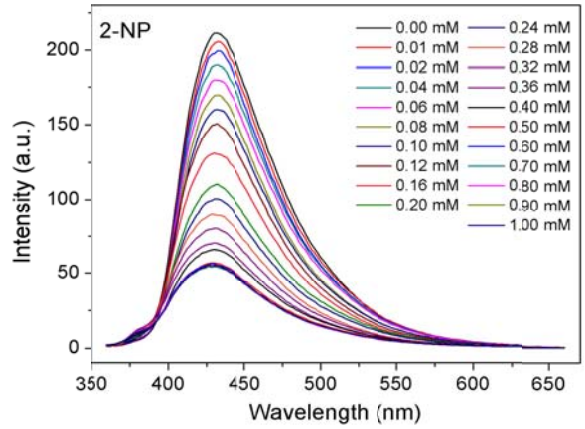
2-NP
Intensity (a.u.)
Wavelength (nm)
0.00 mM
0.01 mM
0.02 mM
0.04 mM
0.06 mM
0.08 mM
0.10 mM
0.12 mM
0.16 mM
0.20 mM
0.24 mM
0.28 mM
0.32 mM
0.36 mM
0.40 mM
0.50 mM
0.60 mM
0.70 mM
0.80 mM
0.90 mM
1.00 mM

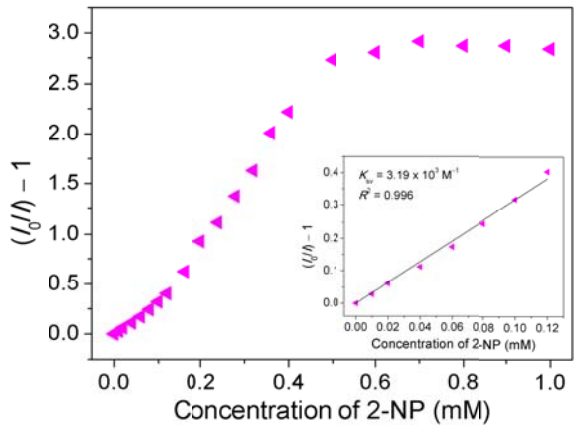
$(I_0/I) - 1$
Concentration of 2-NP (mM)
K_{sv} = 3.19 x 10^3 M^{-1}
R^2 = 0.996

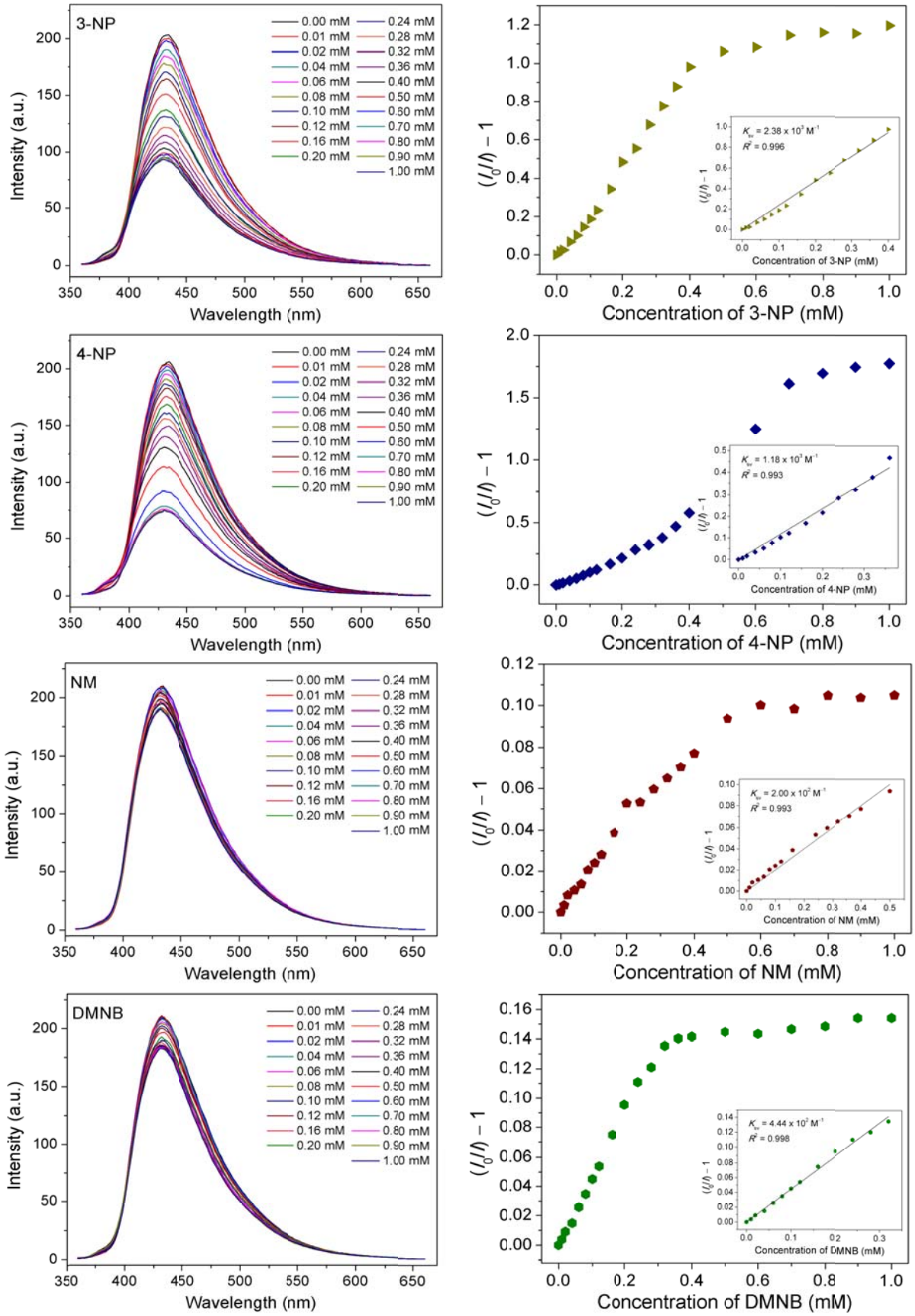

Fig. S10 (Left) Fluorescence responses of **3** in toluene suspension (3.0 mg/3 mL) toward different concentrations of different nitro analyte. (Right) Stern–Volmer plot for nitro analyte in the presence of toluene suspension of **3** in the range from 0 to 1.00 mM. Inset shows the linear region for Stern–Volmer analysis of **3** as a function of concentration of nitro analyte.

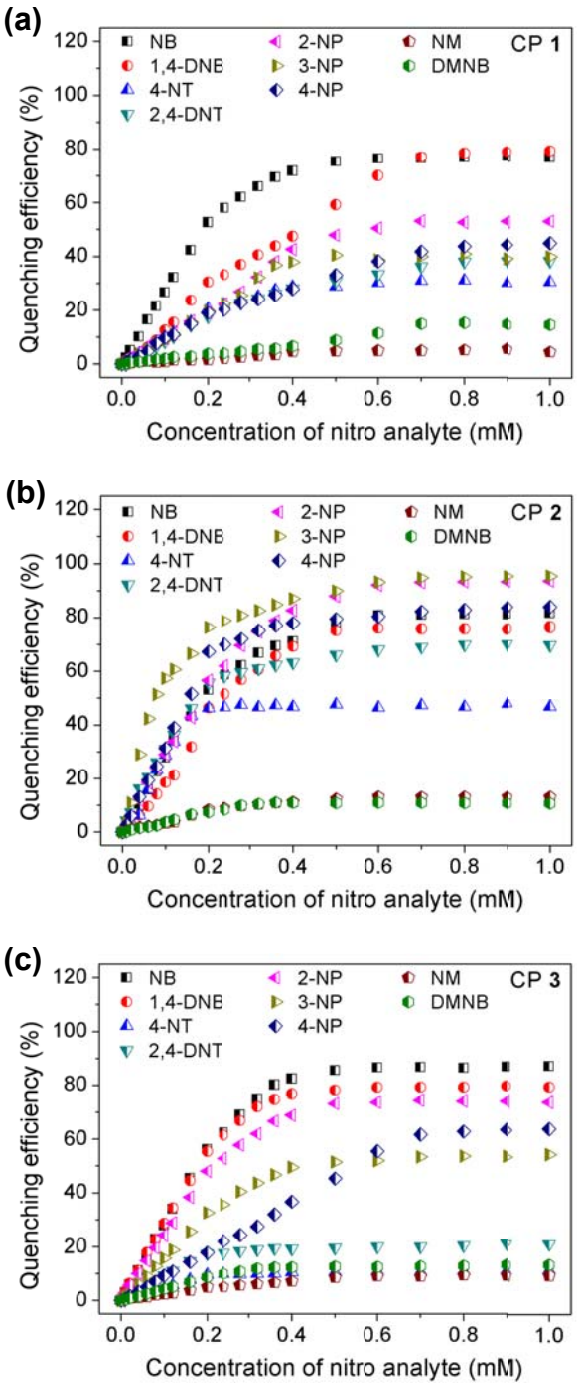

Fig. S11 (a–c) Fluorescence quenching percentage of various nitro analytes at different concentrations (0–1.00 mM) for the toluene suspensions of CPs **1**–**3**.

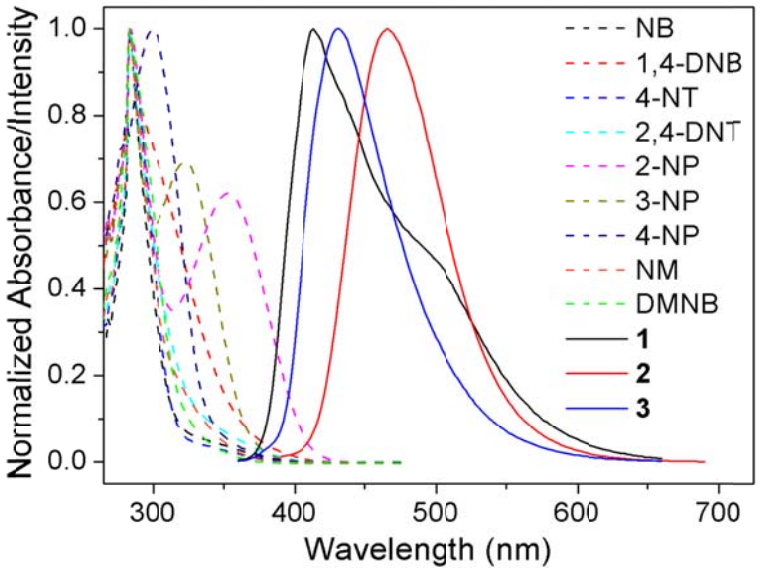

Fig. S12 Normalized UV-Vis spectra of toluene solutions of nitro anal**y**tes and normalized fluorescence emission spectra of toluene suspensions of CPs **1**–**3**.

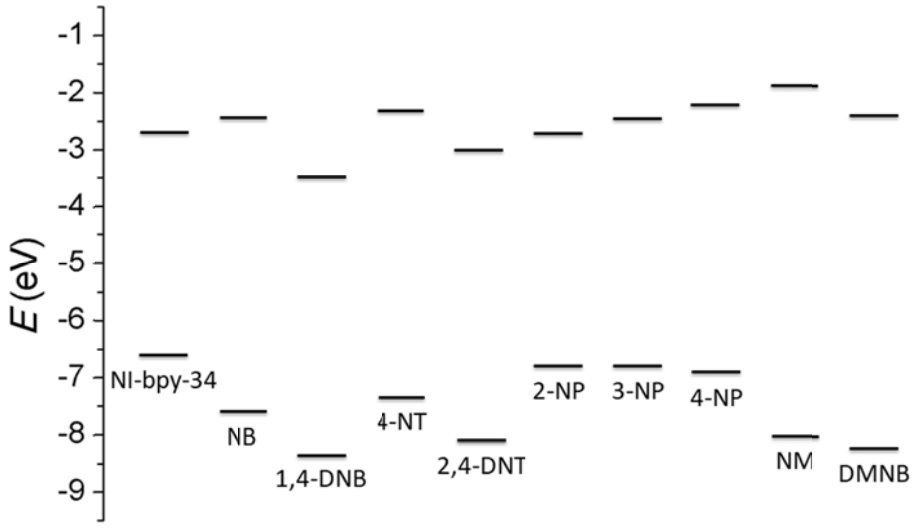

	HOMO (eV)	LUMO (eV)	Energy gap (eV)
NI-bpy-34	-6.6238	-2.7124	3.9114
NB	-7.6007	-2.4324	5.1683
1,4-DNB	-8.3550	-3.4964	4.8586
4-NT	-7.3629	-2.3195	5.0434
2,4-DNT	-8.1098	-2.9777	5.1321
2-NP	-6.7980	-2.7236	4.0744
3-NP	-6.7996	-2.4607	4.3389
4-NP	-6.9226	-2.2232	4.6994
NM	-8.0207	-1.8945	6.1262
DMNB	-8.2271	-2.3878	5.8393

Fig. S13 HOMO and LUMO energies for NI-bpy-34 and nitro analytes.

Measurements of limit of detection (LOD).

LOD measurements were performed at low concentrations of nitro analytes. Fluorescence responses of CPs **1**–**3** (3 mg dispersed in 3 mL of toluene) toward different concentrations of nitro analytes (10−100 μM) in toluene were recorded. LOD was determined using the equation: LOD = 3σ/m, where σ = standard deviation from ten blank measurements for the toluene suspensions of CPs **1**–**3** and m = slope of the linear curve plotted at lower concentration for LOD measurements.

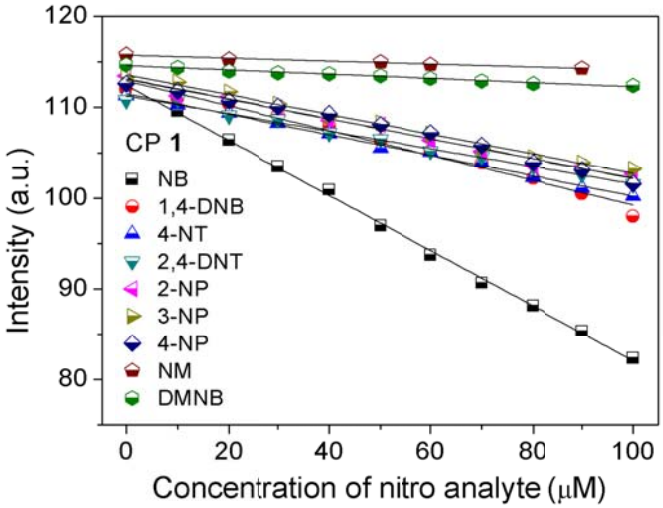

Blank readings	Nitro analyte								
	NB	1,4-DNB	4-NT	2,4-DNT	2-NP	3-NP	4-NP	NM	DMNB
#1	111.8	112.0	111.4	110.9	112.7	112.7	112.5	115.4	113.6
#2	112.0	111.2	111.4	110.9	112.5	113.2	113.2	115.0	114.0
#3	112.1	112.1	110.6	110.1	113.7	112.7	112.7	114.9	113.8
#4	111.5	111.9	111.6	110.7	112.8	112.2	112.0	115.1	113.9
#5	111.8	112.2	111.7	111.1	112.6	113.4	113.0	113.8	113.6
#6	111.6	111.7	111.3	110.5	112.4	112.3	112.4	114.5	113.4
#7	111.1	112.3	111.4	110.5	113.3	112.6	111.8	114.5	113.6
#8	111.4	112.3	111.5	110.7	113.1	112.6	113.1	114.4	113.3
#9	112.0	111.9	110.9	111.4	113.1	113.1	112.9	114.7	114.8
#10	111.3	112.6	110.4	110.3	113.3	112.8	113.1	114.5	113.4
Standard deviation (σ)	0.3340	0.3853	0.4367	0.3843	0.4170	0.3806	0.4855	0.4467	0.4351
Slope (m)	0.3036	0.1368	0.1131	0.09700	0.1089	0.1086	0.1099	0.01614	0.02329
R^2	0.999	0.980	0.996	0.991	0.983	0.992	0.983	0.973	0.981
LOD (3σ/m), μM (ppm)	3.30 (0.41)	8.45 (1.42)	11.58 (1.59)	11.89 (2.16)	11.49 (1.60)	10.52 (1.46)	13.25 (1.84)	83.03 (5.07)	56.05 (9.87)

Fig. S14 Linear region of fluorescence intensity for the toluene suspension of **1** upon incremental addition of nitro analytes in the range from 10 μM to 100 μM. The following table lists the relevant parameters of LOD of the toluene suspension of **1** toward various nitro analytes. Conditions: λ_{em} = 414 nm, λ_{ex} = 280 nm.

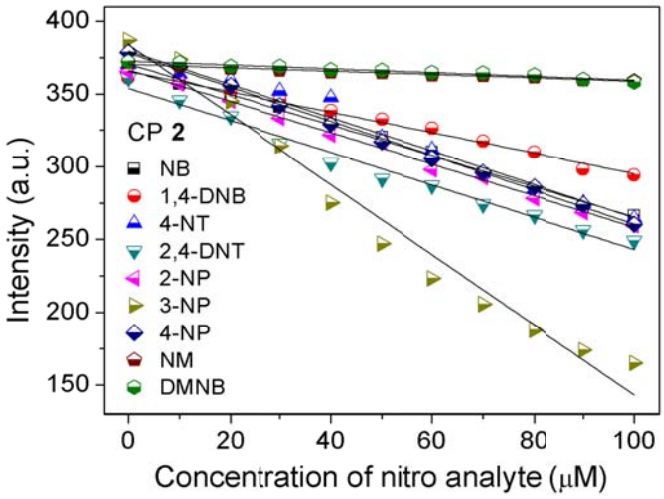

Blank readings	Nitro analyte								
	NB	1,4-DNB	4-NT	2,4-DNT	2-NP	3-NP	4-NP	NM	DMNB
#1	366.6	363.0	369.6	364.2	363.3	385.7	375.4	371.9	368.4
#2	365.5	362.3	367.6	364.2	362.1	387.9	377.3	369.9	371.5
#3	364.4	360.9	370.2	360.5	362.4	387.3	378.0	369.6	373.6
#4	363.7	358.4	370.8	360.0	364.6	386.4	374.7	370.6	370.5
#5	364.4	363.8	369.7	358.9	361.1	384.2	375.6	370.5	373.8
#6	365.4	363.6	367.2	363.5	364.2	382.1	375.1	367.2	372.9
#7	366.9	364.3	368.0	359.8	360.2	383.6	374.5	374.0	372.1
#8	364.3	361.5	368.0	361.5	362.7	383.6	376.5	374.4	375.7
#9	364.2	360.5	367.7	361.6	363.6	387.5	376.1	369.7	371.2
#10	362.4	361.6	369.7	364.8	362.1	386.5	375.1	369.6	373.7
Standard deviation (σ)	1.350	1.795	1.277	2.129	1.358	1.981	1.142	2.170	2.059
Slope (m)	1.0526	0.7036	1.1466	1.1083	1.0819	2.4082	1.1773	0.1160	0.1313
R^2	0.994	0.988	0.971	0.981	0.996	0.972	0.998	0.975	0.964
LOD (3σ/m), μM (ppm)	3.85 (0.47)	7.65 (1.29)	3.34 (0.46)	5.76 (1.05)	3.77 (0.52)	2.47 (0.34)	2.91 (0.40)	56.12 (3.43)	47.06 (8.29)

Fig. S15 Linear region of fluorescence intensity for the toluene suspension of **2** upon incremental addition of nitro analytes in the range from 10 μM to 100 μM. The following table lists the relevant parameters of LOD of the toluene suspension of **2** toward various nitro analytes. Conditions: λ_{em} = 466 nm, λ_{ex} = 280 nm.

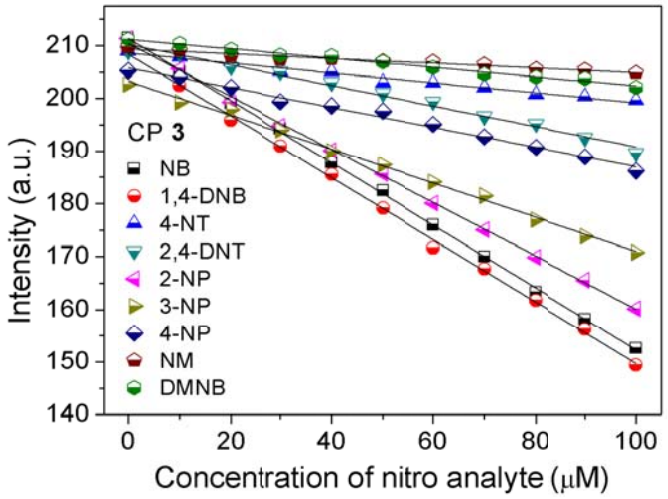

Blank readings	Nitro analyte								
	NB	1,4-DNB	4-NT	2,4-DNT	2-NP	3-NP	4-NP	NM	DMNB
#1	210.7	208.5	207.6	206.2	208.3	200.4	201.9	207.3	209.1
#2	207.7	207.0	205.3	206.5	210.9	200.4	205.8	206.7	206.6
#3	208.5	202.9	205.5	208.6	211.7	202.1	205.3	207.9	207.1
#4	209.4	209.1	206.7	205.2	206.3	207.1	205.5	206.7	208.2
#5	210.1	208.7	207.6	204.3	205.6	202.3	201.8	208.6	206.7
#6	208.2	206.2	207.7	205.5	207.3	206.4	200.9	210.5	206.7
#7	208.1	206.4	207.8	204.1	209.7	199.8	202.9	210.7	205.5
#8	207.8	207.9	207.1	207.0	203.7	203.1	203.2	205.3	206.3
#9	209.5	206.1	205.7	202.9	206.7	208.4	203.6	210.5	208.6
#10	208.8	204.7	205.8	204.1	203.3	202.3	202.1	209.0	207.8
Standard deviation (σ)	1.013	1.933	1.011	1.684	2.834	3.029	1.724	1.865	1.129
Slope (m)	0.5908	0.5872	0.09400	0.1946	0.5036	0.3225	0.1886	0.04436	0.08791
R^2	0.999	0.999	0.979	0.986	0.999	0.997	0.990	0.952	0.989
LOD (3σ/m), μM (ppm)	5.14 (0.63)	9.88 (1.66)	32.27 (4.42)	25.97 (4.73)	16.88 (2.35)	28.18 (3.92)	27.43 (3.82)	126.13 (7.70)	38.53 (6.79)

Fig. S16 Linear region of fluorescence intensity for the toluene suspension of **3** upon incremental addition of nitro analytes in the range from 10 μM to 100 μM. The following table lists the relevant parameters of LOD of the toluene suspension of **3** toward various nitro analytes. Conditions: λ_{em} = 434 nm, λ_{ex} = 280 nm.

Table S2. Comparison of sensing performances toward NB among various CP/MOF sensors

CP/MOF-based sensors	K_{sv}, M^{-1}	LOD, μM (ppm)	Media	Reference
$[Zn_2(1,4\text{-bdc})(1,4\text{-Hbdc})_2(NI\text{-bpy-}34)_2]$ (**1**)	3.63×10^3	3.30 (0.41)	toluene	This work
$[Zn_2(2,6\text{-ndc})(2,6\text{-Hndc})_2(NI\text{-bpy-}34)_2]\cdot H_2O$ (**2**)	6.40×10^3	3.85 (0.47)	toluene	This work
$[Zn(Hbtc)(NI\text{-bpy-}34)(H_2O)]\cdot H_2O$ (**3**)	3.91×10^3	5.14 (0.63)	toluene	This work
$\{[Zn(IPA)(L^1)]\}_n$	1.87×10^3	N.A.	H_2O	S1
$\{[Cd(IPA)(L^1)]\}_n$	1.36×10^3	N.A.	H_2O	S1
$[Zn_2(L^2)(bpy)(H_2O)_2]\cdot(H_2O)_3(DMF)_2$	N.A.	40.6 (5)	CH_3CN	S2
$[Zn_3(L^3)_2(L^4)]$	N.A.	406 (50)	DMF	S3
$[NH_2(CH_3)_2]_2[Cd_{17}(L^5)_{12}(\mu_3\text{-}H_2O)_4(DMF)_2(H_2O)_2]\cdot$solvent	N.A.	1.10 (0.135)	DMF	S4
$[Eu(HL^6)_3(CH_3OH)_2]_n$	2.38×10^4	49 (6.03)	$CHCl_3$	S5
$[Tb(HL^6)_3(CH_3OH)(H_2O)]_n\cdot H_2O$	1.728×10^4	53 (6.52)	$CHCl_3$	S5

Abbreviations: NI-bpy-34 = *N*-(pyridin-3-yl)-4-(pyridin-4-yl)-1,8-naphthalimide; 1,4-H_2bdc = benzene-1,4-dicarboxylic acid; 2,6-H_2ndc = naphthalene-2,6-dicarboxylic acid; H_3btc = benzene-1,3,5-tricarboxylic acid; H_2IPA = isophthalic acid; L^1 = (*E*)-N'-(pyridin-3-ylmethylene)nicotinohydrazide; H_4L^2 = bis-(3,5-dicarboxyphenyl)terephthalamide; bpy = 4,4′-bipyridine; H_3L^3 = 4-[3-(4-carboxyphenoxy)-2-[(4-carboxyphenoxy)methyl]-2-methyl-propoxy]benzoic acid; L^4 = 1,4-bis(1-imidazolyl)benzene; H_3L^5 = 2,4,6-tris[1-(3-carboxylphenoxy)ylmethyl]mesitylene; H_2L^6 = 3-(picolinamido)benzoic acid.

References

(S1) B. Parmar, Y. Rachuri, K. K. Bisht, R. Laiya and E. Suresh, *Inorg. Chem.*, 2017, **56**, 2627–2638.

(S2) G.-Y. Wang, L.-L. Yang, Y. Li, H. Song, W.-J. Ruan, Z. Chang and X.-H. Bu, *Dalton Trans.*, 2013, **42**, 12865–12868.

(S3) M. Guo and Z.-M. Sun, *J. Mater. Chem.*, 2012, **22**, 15939–15946.

(S4) D. Tian, Y. Li, R.-Y. Chen, Z. Chang, G.-Y. Wang and X.-H. Bu, *J. Mater. Chem. A*, 2014, **2**, 1465–1470.

(S5) S. Srivastava, B. K. Gupta and R. Gupta, *Cryst. Growth Des.*, 2017, **17**, 3907−3916.

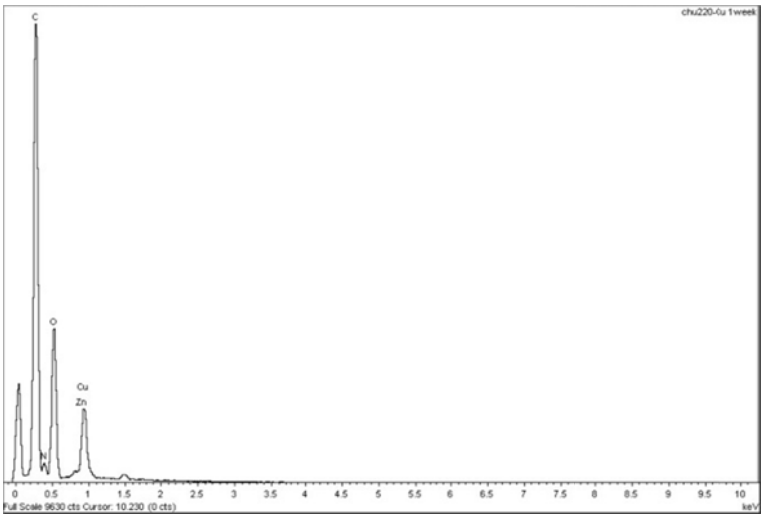

Fig. S17 EDX spectrum of the Cu^{2+}-exchanged greenish crystals of **3** obtained from a metal-ion exchange process for approximate 7 days.

Fig. S18 Time-dependent optical images of **3** during the Cu^{2+} ion exchange process within 30 minutes, showing gradual change in crystal color and maintenance in crystal morphology.